



HAL
open science

Supercritical millifluidic process for siRNA encapsulation in nanoliposomes for potential Progeria treatment (ex-vivo assays)

Mathieu Martino, Adil Mouahid, Michelle Sergent, Camille Desgrouas, Catherine Badens, Elisabeth Badens

► To cite this version:

Mathieu Martino, Adil Mouahid, Michelle Sergent, Camille Desgrouas, Catherine Badens, et al.. Supercritical millifluidic process for siRNA encapsulation in nanoliposomes for potential Progeria treatment (ex-vivo assays). *Journal of Drug Delivery Science and Technology*, 2023, 87, 10.1016/j.jddst.2023.104804 . hal-04254108

HAL Id: hal-04254108

<https://amu.hal.science/hal-04254108v1>

Submitted on 16 Nov 2023

HAL is a multi-disciplinary open access archive for the deposit and dissemination of scientific research documents, whether they are published or not. The documents may come from teaching and research institutions in France or abroad, or from public or private research centers.

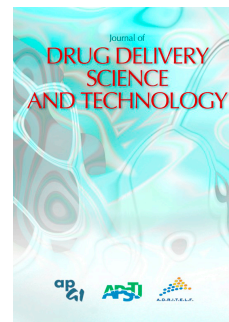
L'archive ouverte pluridisciplinaire **HAL**, est destinée au dépôt et à la diffusion de documents scientifiques de niveau recherche, publiés ou non, émanant des établissements d'enseignement et de recherche français ou étrangers, des laboratoires publics ou privés.

Copyright

Journal Pre-proof

Supercritical millifluidic process for siRNA encapsulation in nanoliposomes for potential Progeria treatment (*ex-vivo* assays)

Mathieu Martino, Adil Mouahid, Michelle Sergent, Camille Desgrouas, Catherine Badens, Elisabeth Badens



PII: S1773-2247(23)00656-1

DOI: <https://doi.org/10.1016/j.jddst.2023.104804>

Reference: JDDST 104804

To appear in: *Journal of Drug Delivery Science and Technology*

Received Date: 20 February 2023

Revised Date: 10 July 2023

Accepted Date: 31 July 2023

Please cite this article as: M. Martino, A. Mouahid, M. Sergent, C. Desgrouas, C. Badens, E. Badens, Supercritical millifluidic process for siRNA encapsulation in nanoliposomes for potential Progeria treatment (*ex-vivo* assays), *Journal of Drug Delivery Science and Technology* (2023), doi: <https://doi.org/10.1016/j.jddst.2023.104804>.

This is a PDF file of an article that has undergone enhancements after acceptance, such as the addition of a cover page and metadata, and formatting for readability, but it is not yet the definitive version of record. This version will undergo additional copyediting, typesetting and review before it is published in its final form, but we are providing this version to give early visibility of the article. Please note that, during the production process, errors may be discovered which could affect the content, and all legal disclaimers that apply to the journal pertain.

© 2023 Published by Elsevier B.V.

1 **Supercritical millifluidic process for siRNA encapsulation in nanoliposomes**
2 **for potential Progeria treatment (*ex-vivo* assays)**

3
4 Mathieu MARTINO¹; Adil MOUAHID¹; Michelle SERGENT²; Camille DESGROUAS^{3,4};
5 Catherine BADENS^{3,4,5}; Elisabeth BADENS¹

6
7 *1 Aix Marseille Univ, CNRS, Centrale Marseille, M2P2, Marseille, 13451, France*

8 *2 Aix Marseille Univ, IMBE, UMR CNRS IRD Avignon Université, Site de l'Etoile, Marseille, France*

9 *3 Aix Marseille Univ, INSERM, MMG, Marseille, France*

10 *4 Aix Marseille Univ, Laboratoire de Chimie Analytique, Faculté de Pharmacie, Marseille, France*

11 *5 APHM, Hôpital de la Timone, Laboratoire de Génétique Moléculaire, 13005 Marseille, France*

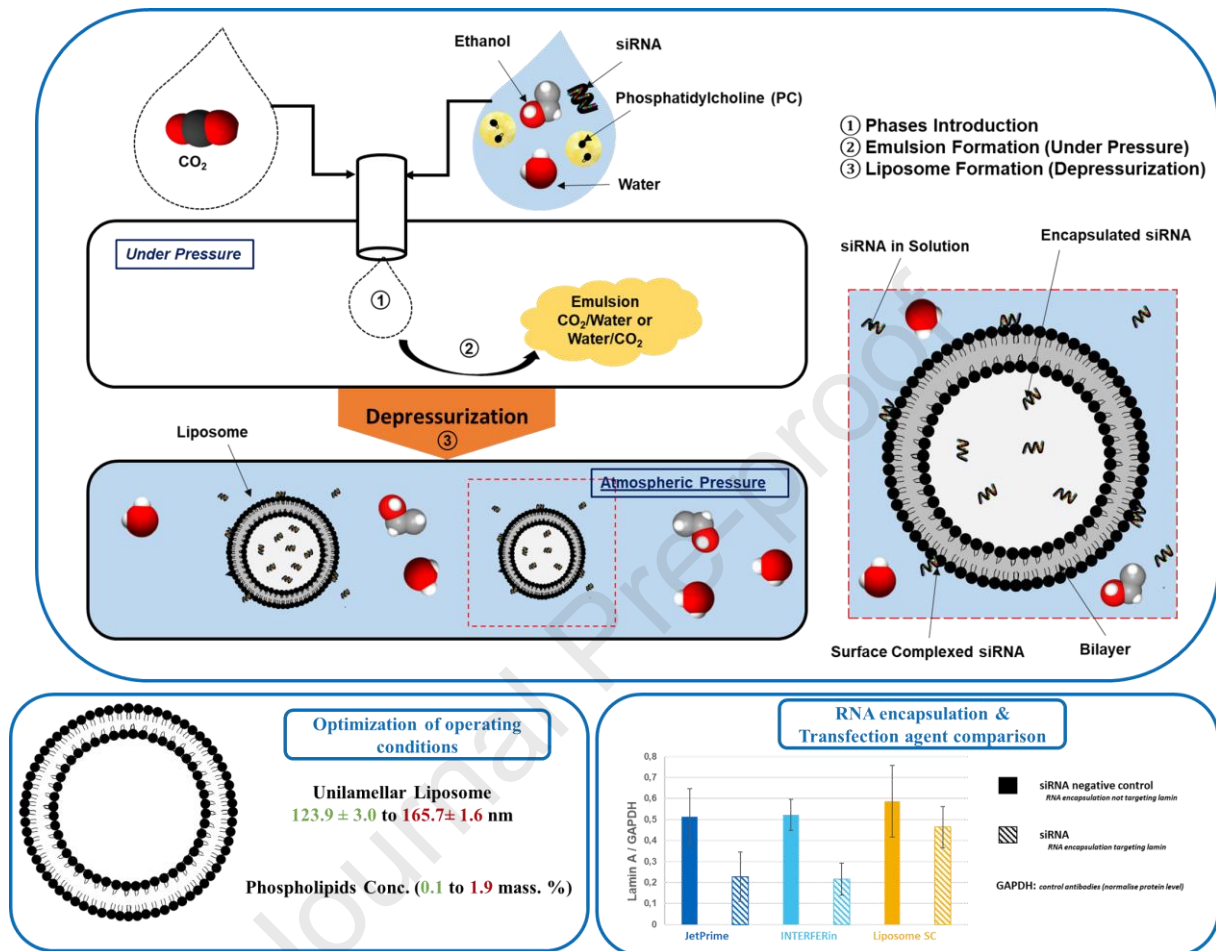
12
13 **Abstract**

14 A millifluidic process working in continuous mode for the preparation of nanoliposomes using
15 supercritical CO₂ has been developed. Nanoliposomes with an average diameter ranging
16 between 123.9 ± 3.0 and 165.7 ± 1.6 nm depending on the operating conditions were obtained.
17 The effects of pressure (90 to 150 bar), temperature (35 to 45°C) and phospholipid mass ratio
18 (0.1 to 1.9 wt%) in feed solution on liposome sizes were investigated. The concentration of
19 phospholipids was found to be the most significant parameter for controlling the mean diameter
20 of nanoliposomes while pressure and temperature had a minor influence on liposomes'
21 properties. The encapsulation of siRNAs targeting the *LMNA* gene by nanoliposomes obtained
22 with the millifluidic process was achieved at optimized operating conditions (150 bar, 35°C and
23 a phospholipid mass ratio in the feed solution of 0.1 wt%). The resulting formulations were
24 compared with commercial transfection agents in *ex vivo* assays. These assays showed a
25 decrease in the expression of the encoded protein lamin A when the formulations obtained with
26 the process developed in this work. Therefore, the use of siRNAs targeting *LMNA*, encapsulated
27 by nanoliposomes represents a potential new therapeutic approach for the treatment of progeria.

32 **Graphical abstract**

33

34



35

36 **Keywords**

37 Nanoliposomes, Supercritical fluids, Process optimization, Millifluidic process, siRNA
 38 encapsulation, Progeria

39

40 **Abbreviation list**

41 **DDS:** Drug Delivery System; **DLS:** Dynamic Light Scattering; **MD:** Mean Diameter; **PDI:**
 42 PolyDispersity Index; **SD:** Standard Deviation; **RNA:** Ribonucleic Acid, **RSM:** Response
 43 Surface Methodology; **siRNA:** Small interfering Ribonucleic Acid; **HGPS:** Hutchinson-
 44 Gilford Progeria Syndrome; **WB:** Western Blot

45

46

47 1. Introduction

48 Since the late 1990s, small new non-coding RNAs have been described which are involved in
49 the regulation of gene expression through a mechanism called RNA interference (RNAi). [1,2].
50 The small-interfering RNAs (siRNAs) represent an alternative to conventional drug therapies
51 targeting disease-related proteins [3,4] as they can specifically inhibit the expression of a gene.
52 Indeed, siRNAs make it possible to modulate the expression of genes by degrading messenger
53 RNAs (encoding the genetic information for the synthesis of proteins in cells), or by inhibiting
54 their translation into proteins. These interfering RNAs are used in particular in cancerology or
55 virology in order to reduce the expression of a specific gene or to inhibit the increase in viral
56 loads [5,6]. The advantage of this type of therapy is linked to specific RNAs targeting,
57 something that allows treatments with fewer side effects [7]. However, siRNAs are very
58 unstable in the organism [8]. They are quickly degraded *in vivo* by the action of ribonucleases
59 and are sensitive to pH variations in the organism [9,10].

60 A possible way to protect nucleic acids following their administration is the use of liposomes,
61 which are soft matter vesicular carriers, non-toxic and biodegradable that can protect RNAs and
62 enhance their delivery [11–15]. The phospholipidic bilayers that mimic cell membranes make
63 liposomes the first choice for encapsulating matrices in therapy [16,17]. The main limitation
64 for the use of liposomes as drug carriers for gene or cancer therapy is their size. Indeed, the
65 particle size is a key characteristic for the particle cellular internalization. Particle with a size
66 up to 5 microns can undergo a cell internalization, but the process is more rapid for particles
67 with a size smaller than 150 nm [18,19]. It is commonly accepted that the recommended particle
68 diameter for treating cancer is in the range of 10-150 nm, and nanoparticles in the range of 10
69 nm penetrate cells more effectively, using pathways of cell internalization which limit
70 degradation.

71 Conventional methods of liposome preparation have been developed for several decades
72 (Bangham method, reverse phase evaporation, solvent injection, detergent) [20–25]. However,
73 these simple techniques require the use of toxic organic solvents. Furthermore, these methods
74 do not allow a good control of the liposome properties (size, size distribution, encapsulation
75 efficiency) [21]. Consequently, the liposomal suspensions formed are relatively unstable. These
76 classical methods are not the most suitable for the preparation of nanoliposomes for siRNA
77 encapsulation.

78 In order to overcome the problems associated with conventional methods, several techniques
79 for liposome formation using supercritical fluids have been developed. Methods based on
80 supercritical fluid, especially supercritical CO₂ (scCO₂), [26] allow the control of the final
81 characteristics of the liposomes forming small vesicles [27–32] with good repeatability. ScCO₂
82 is an interesting alternative to organic solvents as CO₂ is nontoxic, non-flammable and its use
83 has led to the reduction of the quantity of required organic solvent for drug production and
84 formulation. At industrial scale, CO₂ is recycled, enabling a green and compact process with
85 limited or even zero discharges and emissions. Several supercritical processes have been
86 developed with a distinction made based on whether the supercritical fluid is used as a solvent
87 or as an antisolvent for the phospholipids [33]. These processes can operate continuously or in
88 batch mode. Depending on the processes used, the size of the liposomes formed can range from

89 10 nm to 1000 μm and they can have different lamellarities (unilamellar or multilamellar).
90 Among these methods, the most commonly used processes are: Supercritical Reverse Phase
91 Evaporation (scRPE), Depressurization of an Expanded Solution into a Aqueous Media
92 (DESAM), Supercritical Assisted Liposome Formation (SuperLip), Supercritical AntiSolvent
93 (SAS) [26]. The advantages and limitations of these different processes are discussed in the
94 literature [26]. The choice of process is essentially based on the desired characteristics of the
95 liposomes formed.

96

97 The objective of this work was to develop a scCO₂ millifluidic process operating in a continuous
98 mode for the preparation of nanoliposomes with a diameter of less than 150 nm in order to
99 encapsulate siRNAs and to evaluate the efficacy of the formulations to modulate gene
100 expression, following a specific model that could be used as a therapeutical approach.
101 Hutchinson-Gilford progeria syndrome (HGPS) is a rare genetic disease causing premature
102 ageing, growth retardation and heart disease [34] and represents an excellent model of potential
103 gene targeted therapy. The molecular cause of the disease is a mutation of the *LMNA* gene
104 leading to the production of an abnormal protein lamin A called progerin which is toxic and
105 leads to an alteration of the nuclear envelope structure and function [35]. The use of siRNAs to
106 decrease *LMNA* expression is known to reduce the progerin level and nuclei alterations and thus
107 constitutes a potential therapeutic strategy [36]. As the effect of *LMNA*-targeted siRNA can be
108 followed in cell culture by the relative quantification of lamin A after treatment, it is a
109 convenient model to evaluate siRNA encapsulation efficacy and safety [35]. The encapsulation
110 of this siRNA model will allow the study of both the efficiency of the process implemented and
111 the efficiency of the formulations obtained for the treatment of HGPS.

112

113 The development of this millifluidic process is part of a process intensification approach
114 consisting of reducing the size of the installations and in having a more flexible use of the
115 process. Using millimetric tubings as a millifluidic device in place of large high-pressure
116 vessels reduces the investment and operating costs. The production capacity can easily be
117 increased by numbering-up the millifluidic devices. Some scale-up issues such as the change
118 of the formed vesicle size linked to the change of vessel or tubing size can thus be totally
119 avoided. The preparation of liposomes using millifluidic devices with supercritical CO₂ has
120 been implemented and described in the work of Murakami *et al.* [37]. The process described in
121 this latter work for the preparation of liposomes consists of a specific micromixer and a four-
122 pump injection system for introducing the different phases required to form liposomes. The
123 process presented in this work allows the preparation of liposomes in classical commercially
124 available stainless steel tubings and by reducing the size of the compound injection device. In
125 fact, the compounds needed to form liposomes (water and phospholipids) are injected in a single
126 phase constituting the single feed solution of the process. The process therefore requires a single
127 pump to inject the compounds used to prepare the liposome and a second pump to supply the
128 device with CO₂ reducing the total amount of pump required. The resulting process is therefore
129 compact, with reduced CAPEX and OPEX costs.

130

131 The first step of this work was to study the influence of the variation of operating conditions
132 (pressure: 90 – 150 bar, temperature: 35 – 45 °C and phospholipid mass ratio: 0.1 - 1.9 wt%)
133 upon the liposome average diameter (without nucleic acids) using response surface
134 methodology (RSM). RSM is a useful tool allowing the selection of the optimal operating
135 conditions for the formation of nanoliposomes with an adequate size for the targeted
136 application, this being the encapsulation of siRNAs.

137 The second step consisted of the experimental study of the siRNA's encapsulation at the
138 previously selected operating conditions. *Ex vivo* transfection assays were performed to
139 evaluate the efficacy of the formulations in comparison with commercial training kits for the
140 decrease of the expression of lamin A.

141

142 **2. Materials and methods**

143 **2.1 Materials**

144 The source of phospholipids used is L- α -phosphatidylcholine from egg yolk (100% purity,
145 Sigma-Aldrich, Saint-Quentin, France). The phospholipids were solubilized in absolute ethanol
146 (99.8%, VWR, Rosny-sous-Bois, France), and in distilled water directly produced in our
147 laboratories. Carbon dioxide (> 99.7 % purity, Air Liquide France) was used in the millifluidic
148 process. The two types of encapsulated RNA were synthesized by the company Eurogentec
149 (Seraing, Belgium) and provided in a lyophilized form. The first one is a *LMNA*-antisense
150 siRNA duplex that specifically targets the *LMNA* transcript (3'UTR region) with the following
151 sequences:

152 - UUU-UCU-AAG-AGA-AGU-UAU-U99

153 - AAU-AAC-UUC-UCU-UAG-AAA-A99

154 The second one is a siRNA universal negative control with a confidential sequence that does
155 not target any gene (SR-CL005-005, Eurogentec, Fremont, CA, USA). The antisense sequence
156 is a sequence able to bind to the *LMNA* gene and thus modulate the expression of the
157 corresponding protein lamin A/C, which constitutes a potential therapy for the treatment of
158 Hutchinson-Gilford Progeria Syndrome (HGPS) in this study.

159 **2.2 Feed solution preparation**

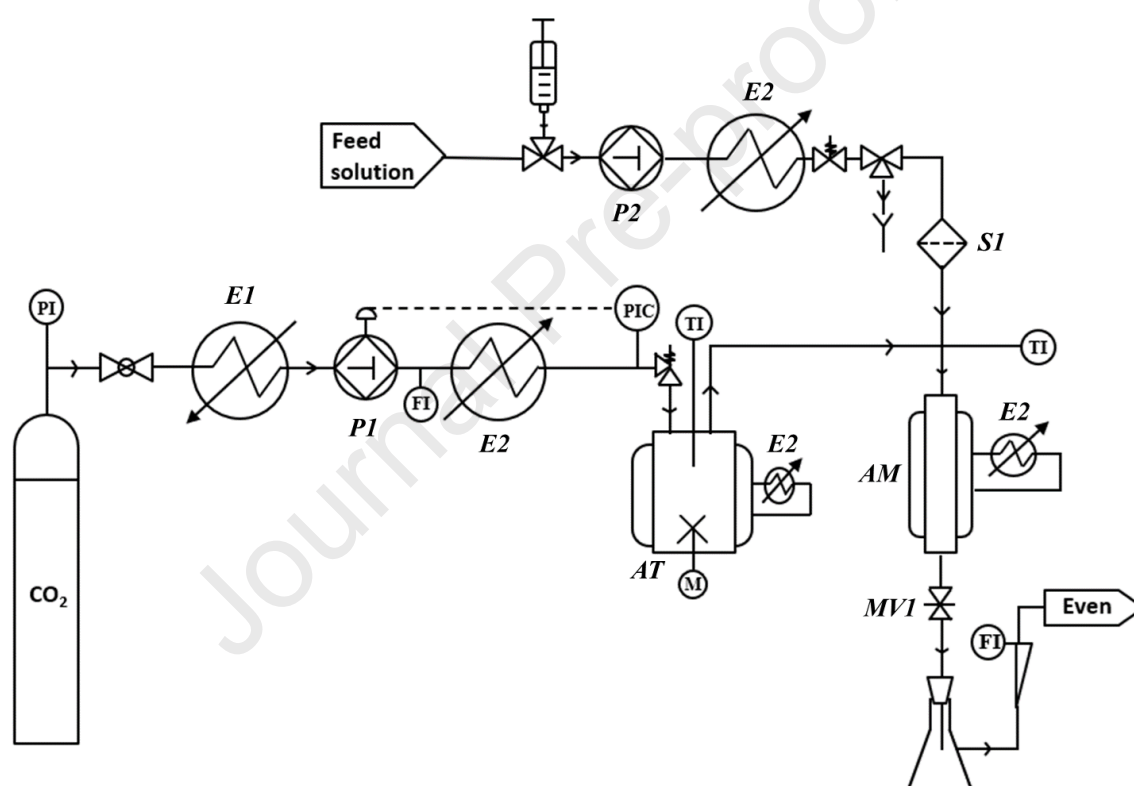
160 The feed solution containing the phospholipids was prepared in a water/ethanol solution
161 (79/21% w/w) at room temperature (20°C). The proportion of water/ethanol has been optimized
162 in previous works [31,38]. In a first step, L- α -phosphatidylcholine (0.3, 2.9 or 5.5 g depending
163 on the desired lecithin mass ratio, respectively 0.1, 1.0 and 1.9 wt%) was dissolved in ethanol
164 (61.5 g). The solution was stirred with a magnetic stirrer until the phospholipids were totally
165 dissolved, then distilled water (228.5g) was added to the solution and stirred again. According
166 to the phosphatidylcholine-ethanol-water phase diagram presented in the work of Söderberg
167 [39], the process feed solution is characterized by the presence of two phases: a liquid phase
168 and a lamellar phase across the entire phospholipid concentration range studied. The feed
169 solutions for RNAs encapsulation were prepared using a phospholipid mass ratio of 0.1 wt%.

170 The RNAs were added to the feed solution to reach a concentration of RNA (*LMNA*-antisense
 171 and negative control) of 5 μM .

172 2.3 Experimental Set-up

173 The continuous millifluidic process experimental set-up is shown in Fig. 1. The stainless-steel
 174 high pressure millifluidic device (AM) is composed of a 1/4" tube (Top Industrie, France) with
 175 an internal volume of 1.2 mL (internal diameter of 3.87 mm, length of 10 cm and
 176 length/diameter ratio of 2.58). This volume reduction allows the formulation of liposomal
 177 suspensions in smaller quantities (useful for the encapsulation of costly molecules). It was
 178 equipped with a double jacket connected to a heating bath circulator (E2) to ensure a
 179 homogeneous working temperature in the whole autoclave. Internal temperature was measured
 180 with a type K thermocouple (TI) inserted into a thermowell.

181



182

183 Fig. 1: Experimental set-up of continuous millifluidic process for nanoliposome preparation (AM: millifluidic device; AT:
 184 buffer autoclave; E1: cold bath circulator; E2: hot bath circulator; MV1: micrometering valve; P1 and P2: liquid high
 185 pressure pump; SI: stainless-steel frit)

186

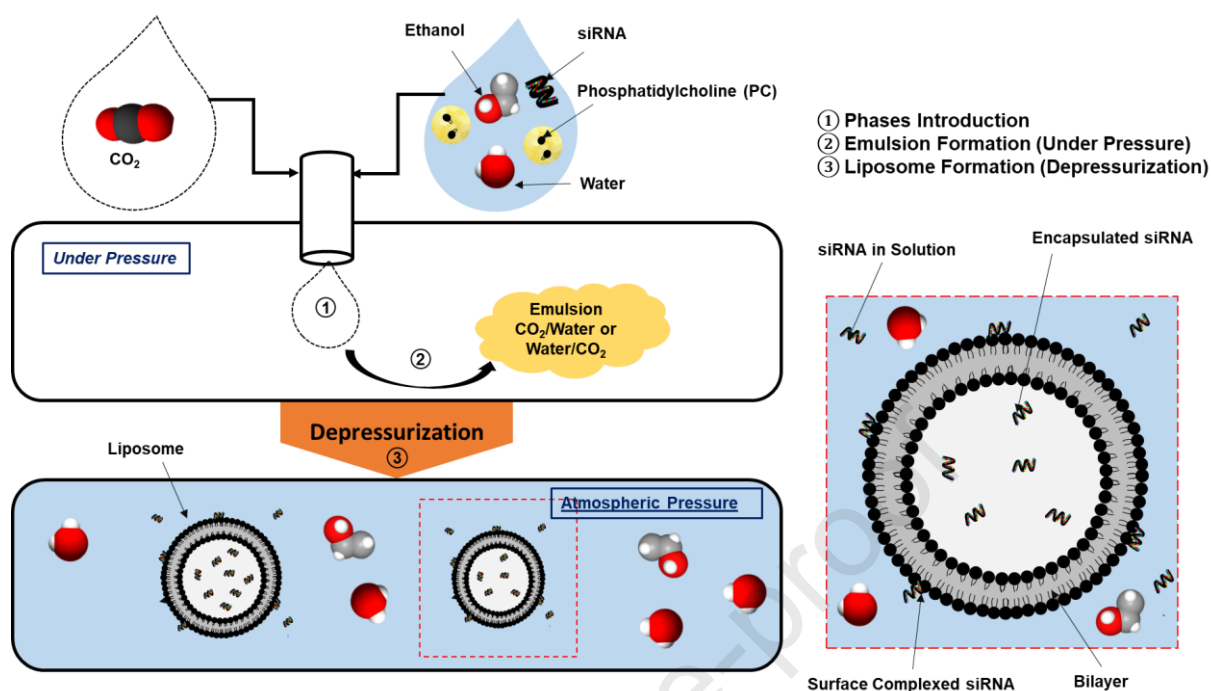
187 CO₂ was primarily cooled thanks to a cold bath circulator (E1) at 0°C to ensure the CO₂ liquid
 188 state before being introduced into the pump. A liquid high-pressure pump (P1 - HPP6/LGP50,
 189 Separex, Champigneulle, France) was used to pressurize CO₂ up to the working pressure (90,
 190 120 or 150 bar). High pressure CO₂ was preheated to the desired temperature (E2) and then
 191 injected into a 0.48 L buffer autoclave (AT – Top Industrie, Vaux-le-Pénil, France) equipped
 192 with a water jacket connected to E2 to ensure constant temperature. The buffer autoclave allows
 193 the supply of scCO₂ into the working millifluidic device (AM) without a sudden change in

194 pressure when the micrometering outlet valve (MV1) is open. A buffer tank is used at industrial
195 scale and placed in the CO₂ recycling loop. Once sc CO₂ was introduced into the millifluidic
196 device (AM) at the working pressure and stabilized at the working temperature (35, 40 or 45°C),
197 the micrometering valve (MV1- connected at its exit to a 1/16" stainless-steel high-pressure
198 tube of 0.5 mm internal diameter) at the outlet of the process was opened to obtain a constant
199 CO₂ flow rate of 8.65 g.min⁻¹. This flow makes it possible to have a continuous process (the
200 heated MV1 valve does not freeze during depressurization). This output flow rate was kept
201 constant during the whole liposome formation protocol. To be able to continuously recover
202 liposomal suspension, the micrometering valve is heated by a heating wire wound on the valve.
203 This heating wire allows to evacuate the ice formed during the expansion of the mixture. This
204 heating wire is left running for the duration of the test (90 min). The system was left to
205 equilibrate for 10 minutes to ensure a constant temperature into the millifluidic device. After
206 equilibrium time, the feed solution was injected through a high-pressure liquid pump (P2 Gilson
207 305, Villiers-le-Bel, France) at a flow rate of 1 mL.min⁻¹. Before being introduced into the
208 device, the pre-heated (E2) feed solution passed through a stainless-steel frit (S1 - 2 μm
209 porosity) placed at the top of the millifluidic device. ScCO₂ and feed solution were injected into
210 the millifluidic device through a T-connection. Upon depressurization of the continuously
211 injected feed solution, the liposomal suspension was recovered in a hermetic Erlenmeyer flask
212 cooled to 0°C by placing it in a water and ice bath. During the production of nanoliposomes,
213 the pressure into the millifluidic device (AM) was maintained constant by the automatic
214 pressure regulation of P1. The CO₂ injection pump (P1) was equipped with a regulation system.
215 The pressure inside the millifluidic device was regulated directly by the P1 pump by increasing
216 or decreasing the CO₂ injection rate to maintain a constant pressure during the test period (90
217 min). When 90 mL of the feed solution was injected, pump P2 was stopped, and pure scCO₂
218 was introduced into AM for 10 min (constant pressure and output flow). ScCO₂ injection was
219 then stopped for complete depressurization. The liposomal suspension formed was recovered
220 and passed through a rotary evaporator at a temperature of 30°C (Laborota 4000, Heidolph,
221 Germany) to evaporate ethanol without degradation of the liposomes formed.

222 A representation of the mechanism of liposome formation in supercritical process is shown in
223 Fig. 2. The aqueous-organic solution containing the phospholipids is injected into the device.
224 This device is previously charged with scCO₂. The injection of the feed solution into scCO₂
225 leads to the formation of a CO₂-in-water or water-in-CO₂ emulsion depending on operating
226 conditions and on the global composition in the millifluidic device [40]. A new type of emulsion
227 appears during depressurization. Indeed, the spontaneous CO₂ release during depressurization
228 induces the formation of a water-in-water emulsion. This emulsion results from the specific
229 organization of phospholipids in water, forming liposomes [40].

230

231



232

233

Fig. 2: Schematic representation of liposome preparation using a supercritical process

234

235 2.4 Liposome characterization

236 Size and size distribution of liposomal suspensions were characterized by a dynamic light
 237 scattering (DLS) instrument (Zetasizer nano S, UK) allowing the measurement of size in the
 238 range of 0.3 nm to 10 000 nm. The mean diameter (MD) associated with Standard Deviation
 239 (SD) was characteristic of liposome size. The polydispersity index (PDI) with its associated
 240 standard deviation was characteristic of liposome size distribution. A He-Ne laser (4 mW, 633
 241 nm) was used as the light source of the Zetasizer instrument. Each sample was measured 5 times
 242 at 25°C in a 10 mm quartz glass cell (Hellma, Germany). An average result was taken for all
 243 experiments and the error bars were determined by calculating the standard deviation of all the
 244 measurements.

245 2.4 Experimental design and response surface methodology

246 The effects of pressure (90 - 150 bar), temperature (35 - 45°C) and phospholipid mass ratio in
 247 the feed solution (0.1 - 1.9 wt%) on the mean diameter (MD) and PDI factor of the
 248 nanoliposomes formed was studied by RSM. Response Y (MD in nm and PDI factor) was
 249 modelled by a second-degree polynomial model given by Eq. 1.

250

$$251 \quad Y = b_0 + b_1 \cdot P + b_2 \cdot T + b_3 \cdot C + b_{1-1} \cdot P^2 + b_{2-2} \cdot T^2 + b_{3-3} \cdot C^2 + b_{1-2} \cdot P \cdot T + b_{1-3} \cdot P \cdot C +$$

$$252 \quad b_{2-3} \cdot T \cdot C \quad (1)$$

253 Where P is the pressure, T is the temperature, C is the phospholipid mass ratio expressed in
 254 unidimensional values and b_i are the modelling coefficients.

255

256 In order to determine the modelling coefficients of the model, a Box-Behnken design was used
 257 and a plan with 13 experiments (Table 1) with 3 levels for each factor was considered. The
 258 three pressure levels considered were 90, 120 and 150 bar, the three temperature levels were
 259 35, 40 and 45°C and the three levels of phospholipid mass ratio in the feed solution were 0.1, 1
 260 and 1.9 wt%. The design and the calculation were performed using AZURAD software
 261 (AZURAD SAS, Marseille, France). The temperature range studied, from 35°C to 45°C, was
 262 chosen in order to work under supercritical conditions. Conducting the process at the lowest
 263 temperature (35°C) makes it possible to study the properties of liposomes at the lowest energy
 264 cost operating conditions. The high temperature (45°C) was set to be able to work with
 265 thermosensitive molecules without the risk of degrading the molecules of interest during their
 266 encapsulation. The pressure range chosen (90 to 150 bar) was also chosen to be in supercritical
 267 conditions. The choice of a range of rather low pressures is in accordance with an energy
 268 optimization approach.

269 *Table 1: Operating conditions for the experimental design*

Experiment	Pressure (bar)	Temperature (°C)	Phospholipid mass ratio (wt %)
1	90	40	1
2	150	35	1
3	90	45	1
4	150	45	1
5	90	40	0.1
6	150	40	0.1
7	90	40	1.9
8	150	40	1.9
9	120	35	0.1
10	120	45	0.1
11	120	35	1.9
12	120	45	1.9
13	120	40	1

270

271 *2.5 Phase composition in the millifluidic device*

272 The phase composition in the millifluidic device was calculated through several steps.

273 The residence times of scCO₂ and of the feed solution were calculated considering the mass
 274 flow rates of scCO₂ (at the operating conditions of pressure and temperature) and of the feed
 275 solution.

276 The mass of scCO₂ flowing through the millifluidic device at working pressure was calculated
277 by using scCO₂ density at the operating conditions (NIST WebBook, National Institute of
278 Standards and Technology, Gaithersburg, Maryland, United States). Knowing the residence
279 time of scCO₂ in the millifluidic device, the mass of scCO₂ flowing through the millifluidic
280 device was calculated.

281 The mass flow rate of the feed solution was calculated, the density of the solution at 25°C being
282 measured. Knowing the mass fraction of water and ethanol in the solution, the mass flow rates
283 of water and ethanol were calculated. Thanks to the residence time of the feed solution in the
284 millifluidic device, it was possible to calculate the mass of water and ethanol flowing through
285 the millifluidic device.

286 The mass fraction of water, ethanol and scCO₂ in the millifluidic device for each experimental
287 condition was then calculated. The mass ratios of phospholipids in the millifluidic device,
288 ranging from 0.05 to 1.0 wt%, were not taken into consideration because their values are much
289 lower than the mass fractions of ethanol, water and CO₂.

290 **2.6 Ex vivo test**

291 *2.6.1 Cell culture*

292 Human control fibroblasts from Institut Coriell (AG07095) were cultured in a complete culture
293 medium (DMEM low glucose (Biowest, Nuaille, France) supplemented with 15% fetal calf
294 serum (Gibco, Loughborough, UK) and 2 mM L-Glutamine (Gibco, Loughborough, UK)) in
295 T25 flasks (Dutscher, Bernolsheim, France) placed in an oven (humid atmosphere, 5% CO₂ and
296 37°C).

297 *2.6.2 siRNA transfection*

298 In order to investigate siRNA transfection, 120 000 cells were seeded with 2 mL of complete
299 medium in wells of a 6-well plate (VWR, Radnor, PA, USA). 24h after plating, 30 nM of siRNA
300 specifically targeting the *LMNA* transcript (3'UTR region) or siRNA not targeting any gene
301 (negative control) were transfected with 3 different vectors:

302 - JetPRIME® which contains a cationic polymer-based molecule acting as encapsulating
303 agent (Polyplus Transfection, Illkirch, France).

304 - INTERFERin® (Polyplus Transfection, Illkirch, France).

305 - Liposomes prepared by supercritical millifluidic process.

306 *2.6.3 Protein extraction*

307 After a siRNA transfection time of 48h, the cells were lysed, and the total proteins extracted by
308 50 µL of 1X extraction buffer. The 3X extraction buffer was prepared by mixing 9.4 mL Tris-
309 HCl pH 6.8; 18.8 mL sodium dodecyl sulfate (SDS) 20%; 15 mL Glycerol; 6.8 mL distilled
310 water and a pinch of Bromophenol Blue. The lysed cells were then collected by scraping into a
311 2 mL Eppendorf tube and sonicated 3 times 0.5 sec ON / 0.5 sec OFF. The total proteins thus
312 extracted were quantified using the Pierce™ BCA Protein Assay kit (ThermoFisher scientific,
313 Waltham, MA, USA).

314 *2.6.4 Western Blot (WB)*

315 The Western blot (semi-quantitative molecular biology analysis method) allowed the detection
 316 of proteins of interest by means of antibodies specific to these proteins. Western blots (WB)
 317 were performed on 40 μg of total protein in the presence of a Chameleon TM Duo Pre-stained
 318 Protein Ladder molecular weight marker (LI-COR Biosciences, Lincoln, NE, USA) on a gel
 319 (Nupage 4-12% Bis-Tris Midi Gel (ThermoFisher scientific, Waltham, MA, USA)). Prior to gel
 320 deposition, proteins were denatured by adding 5% of 2-mercaptoethanol and heating for 5 min
 321 at 95 °C. Migration was performed in a MES buffer (Life Technologies, Carlsbad, California,
 322 USA) at 200V for 1h. The separated proteins were transferred to an Immobilon-FL membrane
 323 (PVDF filter, Chemicon/Millipore, USA). The membrane was then saturated with a fluorescent
 324 WB blocking buffer (#MB-070 (Rockland)) diluted $\frac{1}{2}$ in 1X TBST (1X TBS prepared from 20x
 325 TBS (Thermo, 28358 Pierce™ 20X TBS Buffer) + 0.1% tween 20). The hybridization of
 326 primary antibodies was performed at room temperature with shaking for 1.5 hr: mouse-derived
 327 monoclonal anti-lamine A/C IgG antibodies (sc-376248, Santa Cruz Biotechnology Inc., Santa
 328 Cruz, CA, USA) diluted at 1:5000 and mouse-derived monoclonal anti-GAPDH IgG antibodies
 329 (MAB374, Merck Millipore, Darmstadt, Germany) diluted at 1:40,000. After three 5-min
 330 washes with 1X TBST under agitation, the secondary antibodies were incubated at room
 331 temperature (20°C) for 45 min under agitation: fluorochrome IRDye®800CW donkey anti-
 332 mouse IgG (926-32212, LI-COR Biosciences, Lincoln, NE, USA) diluted at 1:15,000.
 333 Fluorescence signals were detected on a Biorad ChemiDoc MP reader according to the
 334 manufacturer's recommendations. Relative quantification of the bands obtained for lamin A
 335 versus the housekeeping protein GAPDH were performed on ImageLab 6.1 (2020, Bio-Rad,
 336 Laboratories, Inc., Hercules, California, USA). All the *ex vivo* experiments were performed in
 337 triplicate.

338 3 Results and discussion

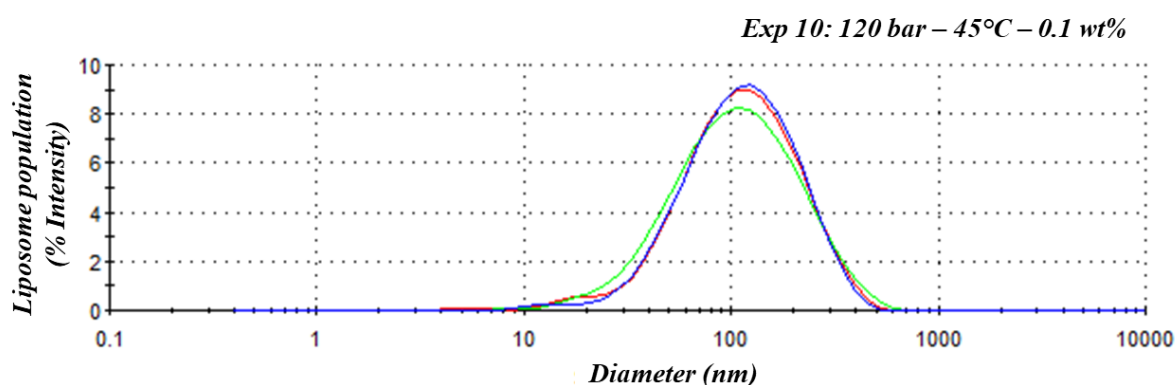
339 3.1 Repeatability test

340 The repeatability was studied by replicating three times the experiment conducted at 120 bar,
 341 45°C with phospholipid mass ratio in the feed solution of 0.1 wt%. The repeatability was
 342 evaluated considering the MD, the size distribution and the PDI factor curves of the liposomes
 343 formed. The results, reported in Table 2 and Fig. 3, show a satisfying repeatability of the
 344 process: the liposomes formed have a mean diameter of 130 nm distributed unimodally.

345 *Table 2: Mean Diameter and PDI of liposome obtained during repeatability test*

Experiment	Mean	Size Distribution	PDI \pm SD
	Diameter (MD) \pm SD (nm)		
10-1	130.6 \pm 3.3	Unimodal	0.292 \pm 0.001
10-2	128.9 \pm 8.6	Unimodal	0.33 \pm 0.06
10-3	129.9 \pm 1.1	Unimodal	0.276 \pm 0.006

346



347

348 *Fig. 3: Size distribution obtained in repeatability tests for continuous millifluidic process*

349

350 **3.2 Operating conditions optimization of the millifluidic device**351 **3.2.1 General findings**

352 The MD, particle size distribution and PDI factor are given in Table 3. The liposomes formed
 353 with the continuous millifluidic process were all found to be unimodally distributed with mean
 354 diameters ranging from 124 nm to 166 nm.

355 *Table 3: MD, size distribution and PDI factor of the formed liposomes at the studied experimental conditions*

Experiment	P (bar)	T (°C)	C (wt %)	MD ± SD (nm)	Size Distribution	PDI ± SD
1	90	40	1	154.6 ± 7.0	Unimodal	0.425 ± 0.001
2	150	35	1	147.2 ± 3.6	Unimodal	0.298 ± 0.003
3	90	45	1	123.9 ± 3.0	Unimodal	0.426 ± 0.001
4	150	45	1	143.0 ± 2.4	Unimodal	0.384 ± 0.002
5	90	40	0.1	130.0 ± 1.4	Unimodal	0.269 ± 0.002
6	150	40	0.1	125.8 ± 0.8	Unimodal	0.254 ± 0.002
7	90	40	1.9	148.4 ± 0.5	Unimodal	0.37 ± 0.08
8	150	40	1.9	155.6 ± 2.2	Unimodal	0.306 ± 0.003
9	120	35	0.1	131.1 ± 1.6	Unimodal	0.28 ± 0.02
10	120	45	0.1	130.6 ± 3.3	Unimodal	0.292 ± 0.001
11	120	35	1.9	165.7 ± 1.6	Unimodal	0.37 ± 0.03
12	120	45	1.9	146.5 ± 2.3	Unimodal	0.31 ± 0.03
13	120	40	1	134.0 ± 3.9	Unimodal	0.33 ± 0.04

356

357 From experimental results for MD and PDI, the polynomial coefficients of Eq. 1 were
358 determined by multilinear regression and are given in Table 4.

359 *Table 4: Regression coefficients of the polynomial model and analysis of the variance for the effects of pressure, temperature,*
360 *and phospholipid mass ratio on the MD and PDI factor of formed liposomes (* $p < 0.05$, ** $p < 0.01$, and *** $p < 0.001$)*

Coefficients	MD	Standard deviation for MD	p-Value for MD	PDI	Standard deviation for PDI	p-Value for PDI
b ₀	139.928	0.792	-	0.34327	0.03148	-
b ₁ (P)	-0.579	0.334	0.22469	-0.03823	0.01326	0.03447*
b ₂ (T)	-7.477	0.338	0.00203**	0.00138	0.01343	0.92210
b ₃ (C)	12.055	0.287	<0.00100** *	0.03145	0.1141	0.03999*
b ₁₋₁ (P-P)	2.235	0.587	0.06265	0.02096	0.02336	0.41070
b ₂₋₂ (T-T)	3.362	0.592	0.02960*	0.03142	0.02353	0.23923
b ₃₋₃ (C-C)	-0.732	0.528	0.29997	-0.06241	0.02099	0.03104*
b ₁₋₂ (P-T)	8.494	0.579	0.00461**	0.03084	0.02302	0.23806
b ₁₋₃ (P-C)	2.85	0.427	0.02174*	-0.01150	0.01699	0.52846
b ₂₋₃ (T-C)	-5.241	0.383	0.0053**	-0.01810	0.01524	0.28824

361

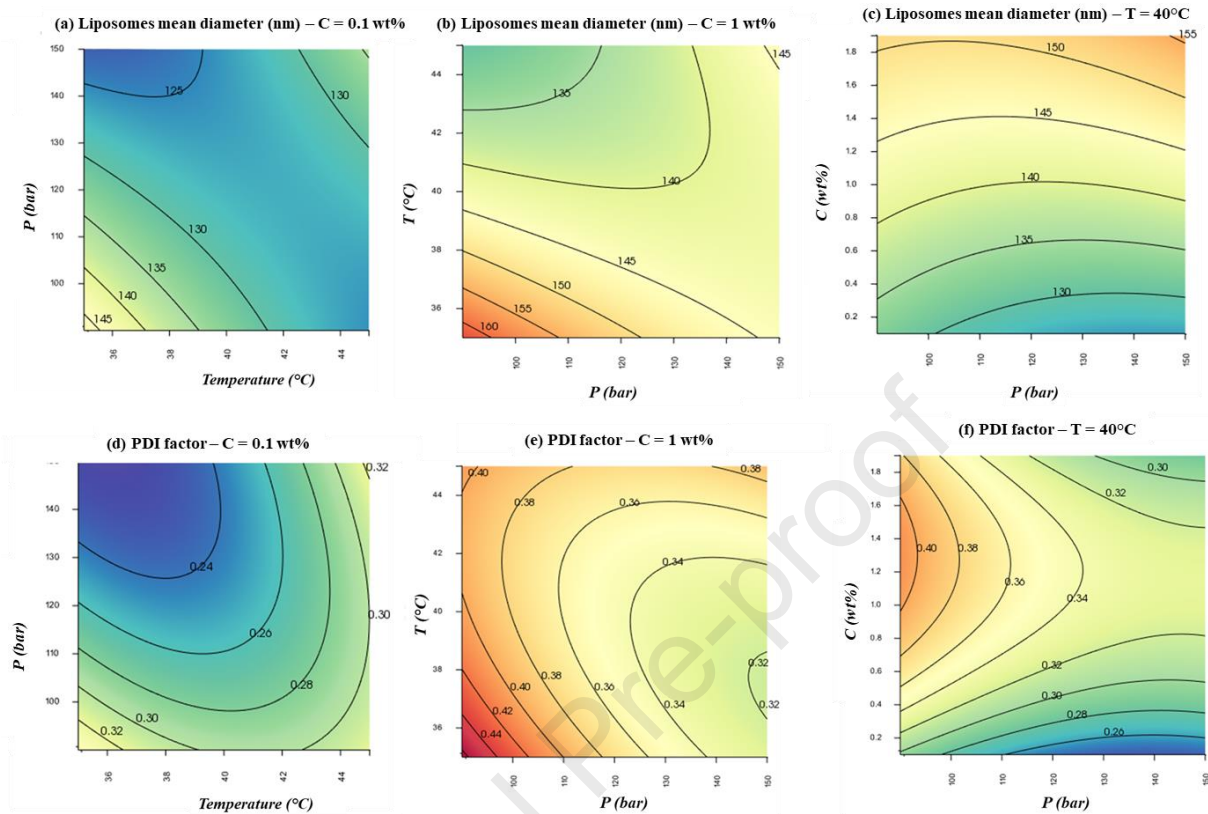
362

363 3.2.2 Influence of the variation of operating conditions

364 For synthesis, the effects of operating condition variations are given in Fig. 4. The effect of
365 pressure on the liposome MD is shown in Fig. 4 (a – c). In general, at a set phospholipid mass
366 ratio and set temperature, an increase in pressure led to a decrease in the liposome MD.
367 Nevertheless, these MD variations occur in a part of the experimental domain (temperature and
368 phospholipids mass ratio), while in the other part of the experimental domain, the MD are not
369 impacted by the pressure variation. For example, on Fig. 4 (a), an increase in pressure from 90
370 to 150 bar at a temperature of 35°C led to a decrease in the liposome MD from 145 nm to 125
371 nm. Fig. 4 (a-b) exhibits large areas where no variations of the liposome MD were observed, as
372 for in the blue and yellow areas shown in Fig. 4 (a) and (b) respectively. Finally, in Fig. 4 (c)
373 whatever the phospholipid mass ratio at a set temperature of 40°C, an increase in pressure from
374 90 to 150 bar did not lead to a variation of liposome MD. These observations suggest that the
375 pressure had a slight influence on the MD of liposomes for given operating conditions, but most
376 of the time, the pressure had no significant effects on the liposome MD which is supported by
377 the p-value of pressure parameter (Table 4) which is greater than 5 % (22.469 %). Moreover,
378 in view of the modelling results and surface plots obtained, the pressure does not have a
379 significant influence in comparison to the effect of phospholipid mass ratio on liposome MD.

380 The effect of pressure on the PDI factor is given in Fig. 4 (d – f). These figures highlight that
381 contrarily to the liposome MD, pressure has an impact on the PDI factor. Indeed, whatever the
382 set parameter, an increase of pressure led to a significant decrease of the PDI factor in the

383 overall experimental domain suggesting a tighter size distribution since only unimodal
 384 distributions were obtained for all operating conditions.



385
 386 Fig. 4: Response surface plots of formed liposomes MD (a) at a set phospholipid mass ratio of 0.1 wt%, (b) at a set
 387 phospholipid mass ratio of 1 wt%, (c) at a set temperature of $T = 40^{\circ}\text{C}$ and PDI factor (d) at a set phospholipid mass ratio of
 388 0.1 wt%, (e) at a set phospholipid mass ratio of 1 wt%, (f) at a set temperature of $T = 40^{\circ}\text{C}$ as function of pressure,
 389 temperature and phospholipid mass ratio in the feed solution

390
 391 To deepen these observations, the mass fractions of water, ethanol and scCO₂ flowing through
 392 the millifluidic device were calculated and reported in Table 5. It was found that the mass
 393 fractions of water (ranging from 43.33 to 58.37 wt%) were always the highest compared to
 394 ethanol and scCO₂ mass fractions. This highest amount corresponds to a two-phase system in
 395 the millifluidic device: a water-rich phase and a CO₂-rich phase. Indeed, the compositions in
 396 the millifluidic device were compared with the CO₂-ethanol-water phase diagram proposed in
 397 the work of Durling *et al.* [41] for a temperature of 40°C and pressures of 100, 200 and 300 bar.
 398 For all the operating conditions of pressure and temperature tested in the experimental design,
 399 two distinct phases are present in the millifluidic device after mixing of the different
 400 compounds. Being largely in the "two-phase" zone of the diagram and not at the limit of the
 401 zone, a slight variation in temperature around 40°C may not significantly affect the number of
 402 phases in presence in the millifluidic device. The proportion of scCO₂ in the millifluidic device
 403 varies according to the operating conditions of pressure and temperature. The mass fraction of
 404 scCO₂ ranged from 25.92 wt% (45°C and 90 bar) to 45.01 wt% (35°C and 150 bar).

405

406 Table 5: Phase mass fractions flowing through the millifluidic device

Temperature (°C)	P (bar)	Water (wt%)	EtOH (wt%)	scCO ₂ (wt%)
35	90	48.91	13.16	37.93
	120	45.04	12.12	42.84
	150	43.33	11.66	45.01
40	90	53.89	14.50	31.61
	120	46.62	12.55	40.83
	150	44.40	11.95	43.65
45	90	58.37	15.71	25.92
	120	48.52	13.06	38.42
	150	45.59	12.27	42.14

407

408 The highest fractions of scCO₂ flowing through the millifluidic device were found for the
409 highest pressures. This observation can be correlated with the evolution of the PDI factor with
410 increasing pressure: the higher the amount of scCO₂ in the millifluidic tube during phospholipid
411 injection, the tighter the size distribution of the liposomes formed. Similar results were observed
412 in the work of Zhao *et al.* [42]. In this present work, the correlation between pressure and size
413 distribution is consistent since the liposomes are formed during the depressurization. Indeed, at
414 high pressures, the depressurisation takes place with a greater pressure drop compared to lower
415 processing pressures. As a result, the expansion of the emulsion during depressurization is more
416 brutal because the quantity of CO₂ released is greater. Therefore, the release of a higher amount
417 of CO₂ leads to the formation of liposomes with narrower size distributions and lower PDI
418 factors due to a faster organization of the phospholipids into liposomes with a more brutal
419 separation of the CO₂. Indeed, a higher process pressure corresponds to a higher pressure drop,
420 leading to enhanced mass transfers during the liposome formation. Therefore, a higher
421 processing pressure resulted in a better uniformity of the liposomes.

422 The effect of temperature is given in Fig. 4 (a-b): at a set phospholipid mass ratio and pressure,
423 an increase in temperature led to a decrease in liposome MD. This effect is more pronounced
424 when the phospholipid mass ratio is 1 wt% (Fig. 4 (b)). At the lowest phospholipid mass ratio
425 (Fig. 4 (a)), the variation on liposome MD with increasing temperature is negligible when the
426 pressures are higher than 125 bar. According to Fig. 4 (a), the liposomes with the smallest MD
427 (125 nm represented by the blue area) are formed at the lowest phospholipid mass ratio when
428 the temperature is close to 35°C and the pressure higher than 130 bar. And according to Fig. 4
429 (b), the liposomes with the smallest MD (135 nm represented by the green area) are formed at
430 the highest phospholipid mass ratio when the temperature is close to 42°C and the pressure
431 higher than 120 bar. These variations suggest that the phospholipid mass ratio should also be
432 considered with temperature variations. On Fig. 4 (d-e) the variations of temperature, whatever
433 the set operating conditions, did not lead to a significant variation of the PDI factor. As a result,
434 temperature and phospholipid concentration have an impact on the average size of the
435 liposomes (as seen in Table 4). However, temperature has no impact on the size distribution
436 (PDI value) of the liposomal suspensions formed.

437

438 The influence of the variations of phospholipid mass ratio upon liposome MD is given in Fig.
439 4 (c). At a given pressure and temperature, increasing the phospholipid mass ratio led to an
440 increase in the liposome MD in the overall experimental domain from 130 to 150 nm.
441 Considering the previous observations on temperature and pressure effects and the p-value in
442 Table 4, phospholipid mass ratio appears to have a very significant effect on the liposome MD.
443 These observations can be explained with the nature of the phases in the Winsor system.
444 Depending on the system studied, there may be the presence of either a single phase, two phases
445 (CO₂-in-water emulsion or water-in-CO₂ emulsion) or three phases (water-rich, CO₂-rich and
446 mid-phase emulsion). These Winsor systems are systems where water and CO₂ are introduced
447 in the same quantities and where the surfactant is introduced at different concentrations. The
448 ternary pressurized system Water/CO₂/Surfactant can have one or more phases depending on
449 the operating conditions (temperature, pressure). The different behaviors of the phases as a
450 function of the surfactant concentration and the operating conditions (temperature and pressure)
451 are described in Fig. 5. Four types of behavior can be observed. According to the notations
452 introduced by Winsor, the first observable behavior is type I (or $\underline{2}$) where the surfactant has a
453 better affinity with CO₂. Therefore, the CO₂ in Water microemulsion is in equilibrium with a
454 water-rich phase. This microemulsion appears as normal micelles. The second observable
455 behavior is the type II (or $\bar{2}$) behavior and describes a system where the Water in CO₂
456 microemulsion in the form of reverse micelles is in equilibrium with a CO₂ rich phase. The
457 third Winsor behavior (type III) describes a three-phase system where the microemulsion is in
458 equilibrium between a CO₂-rich phase and a water-rich phase. Finally, the last Winsor system
459 (type IV behavior) is characterized by the presence of a single phase containing the
460 microemulsion.

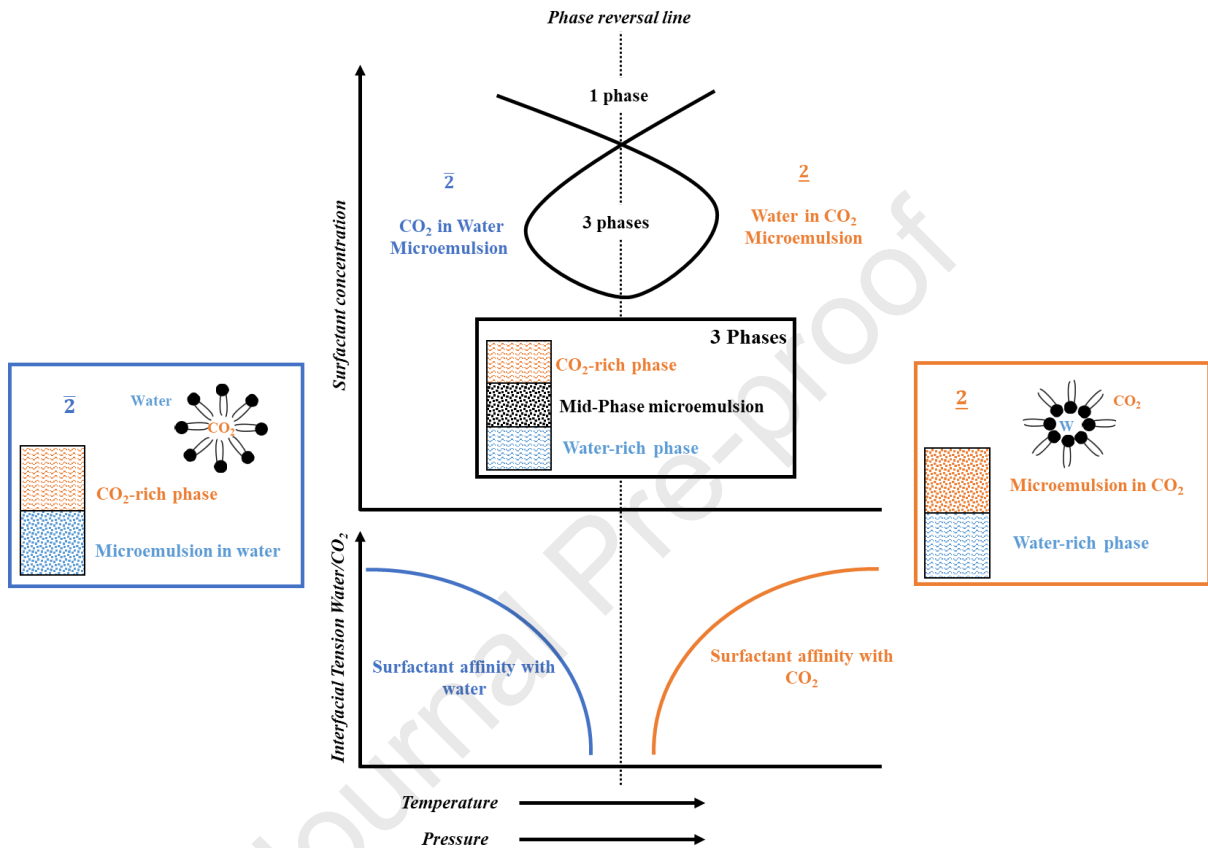
461

462 The behaviour of the system under pressure is directly related to the concentration of the
463 surfactant (here phospholipids). The use of higher surfactant contents leads to an increase in the
464 diameter of the micelles formed. The work of Lesoin *et al.* [40], based on observations of
465 emulsions under pressure and on granulometric analyses, shows that the higher the water/lipid
466 mass ratio, the smaller the diameter of the liposomes formed and vice versa. For the same
467 amount of water in the autoclave, the increase in phospholipid concentration induces an increase
468 in the average diameter of the liposomes formed. Table 5 shows that over the whole operating
469 range, the water compositions in the autoclave for the batch process do not vary significantly.
470 Based on the work of Lesoin *et al.* [40], the increase in liposome size can be directly correlated
471 to the increase in phospholipid content. These observations can be explained by the nature of
472 the phases present in the autoclave as a function of the surfactant (phospholipid) concentration.
473 The significant effect of the phospholipid mass ratio can also be explained by the increase in
474 phospholipid mass ratio flowing through the millifluidic device which can lead to a change in
475 the equilibria of the emulsions under pressure. This change has been studied by Lesoin *et al.*
476 [40] who showed that the higher water/phospholipid ratio allows the preparation of liposomes
477 with the smallest diameter. Therefore, as the mass fraction of water flowing through the
478 millifluidic device was systematically about 50 wt%, the increase in phospholipid concentration

479 directly induces an increase in liposome size. The increase in liposome size with the
 480 concentration of phospholipids was also observed by Reverchon *et al.* [43]. The higher
 481 phospholipid content promotes contact between the phospholipids, resulting in the organisation
 482 of several bilayers, forming multilamellar liposomes.

483

484



485

486 Fig. 5: Winsor systems as a function of surfactant concentration, interfacial tension and operating conditions of temperature
 487 and pressure

488

489 The influence of the variations of phospholipid mass ratio upon the PDI factor is shown in Fig.
 490 4 (f). Increasing the phospholipid mass ratio up to about 1.1 % at set pressures and temperatures
 491 leads to an increase in the PDI factor (from 0.28 to 0.38 at 100 bar and 40°C). At higher mass
 492 ratio, no variations of the PDI factors were observed (about 0.38 at 100 bar and 40°C). The
 493 lowest PDI factor (0.26) was found at the lowest phospholipid mass ratio.

494 Considering these overall results, the optimal operating conditions allowing the formation of
 495 liposomes with the smallest MD and the smallest size distribution (lowest PDI value) is 150
 496 bar, 35°C and a phospholipid mass ratio of 0.1 wt% in the feed solution. In order to confirm the
 497 predictive model of MD and PDI of liposomes, a test with these operating conditions was
 498 carried out. When using the millifluidic process at these optimized operating conditions, the
 499 liposomes obtained in the liposome's suspensions are distributed in a unimodal population with
 500 a PDI of 0.245 ± 0.003 with average diameters of 125.2 ± 2.2 nm. The results obtained are in

501 good agreement with the defined mathematical model and confirm the validity of the model in
502 the studied operating area.

503 **3.3 siRNA encapsulation and transfection assay**

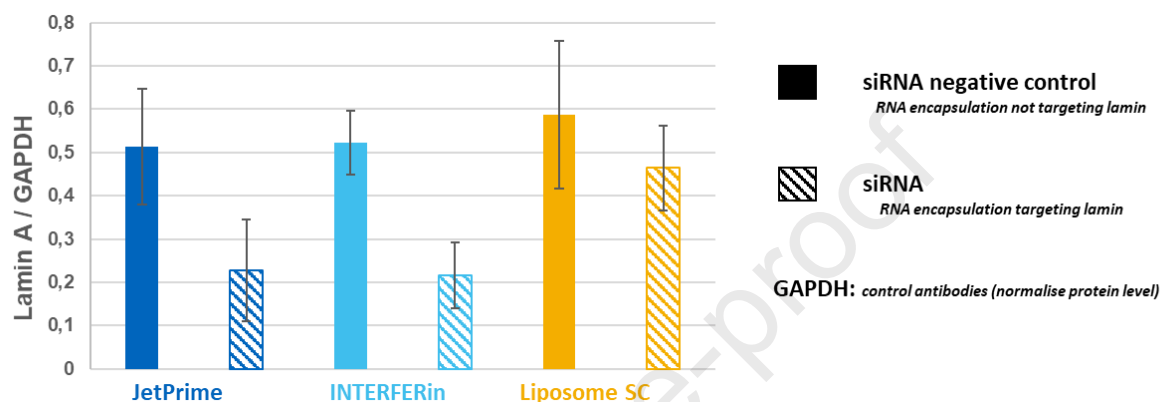
504 Encapsulated siRNAs targeting *LMNA* represent an innovative therapeutic approach for the
505 treatment of progeria. Two different siRNAs were encapsulated using the millifluidic device: a
506 siRNA specifically targeting the *LMNA* transcript (siLMNA) and a siRNA non-targeting any
507 gene (Control) allowing the comparison of the results of the different formulations. The
508 experiments were carried out at the optimal operating conditions established in the previous
509 sections: 150 bar, 35°C and a phospholipid mass ratio in the feed solution of 0.1 wt% in the
510 operating area studied.

511 Using these operating conditions, liposomes with MD ranging between 120 and 130 nm were
512 produced (liposomes diameters were respectively 125.2 ± 2.2 nm without siRNA and $123.6 \pm$
513 4.4 nm with siARN) The mean diameter of the liposomes obtained is similar with or without
514 siRNA encapsulation. The liposomal suspensions recovered at the end of the process had a
515 siRNA concentration of 5 μ M (for siLMNA and Control). After ethanol removal by rotavapor,
516 the siRNA concentrations in the liposomal suspensions increased to 6.5 μ M. These
517 concentrations correspond to the amount of RNA in the feed solution. The ethanol-free
518 liposomal suspensions were used to treat cells in culture at a final concentration of siRNAs of
519 30 nM, and lamin A expression in these cells was quantified by WB. The expression of the
520 housekeeping protein GAPDH was also quantified as a loading control because it is
521 constitutively expressed in almost all tissues in high amounts. The results are shown as lamin
522 A/GAPDH ratio to allow the comparison of the different transfection agents (JetPrime;
523 INTERFERin and liposomes prepared in supercritical medium). In all conditions, the effect of
524 the *LMNA*-targeted siRNA was compared to the effect of the control.

525 The results, presented in Fig. 6, show the decrease in lamin A expression when using all three
526 transfection agents. The lamin A/GAPDH ratio decreased from 0.51 to 0.23 between control
527 and RNA assays for JetPrime, from 0.52 to 0.22 for INTERFERin and from 0.59 to 0.46 for
528 supercritical liposomes. However, the decrease in lamin A expression was only significant for
529 the JetPrime and INTERFERin assays. Indeed, the decrease observed for the assays when using
530 liposomes is only a trend as it remains within the error range of the measurements. However,
531 the use of liposomes as transfection agents appears to have a major advantage over the other
532 two agents. Indeed, transfections performed with liposomes were much less toxic for the cells
533 than transfections performed with commercial vectors (JetPrime and INTERFERin). The
534 toxicity of the formulations was not quantified but simply carried out with visual observations
535 during the transfection assays. It is important to underline that the formulations developed in
536 this work enabled WB results coherent with the results obtained with the two other commercial
537 vectors even if the lamin A/GAPDH ratios obtained are higher than for the two commercial
538 vectors. These results demonstrate that the cells were not damaged by the formulations and that
539 the liposomes formed by the supercritical millifluidic process developed during this study can
540 be used to develop effective formulations for siRNA transfection. The advantage of this process
541 is that it can be used to produce formulations for patients, either small batches for a clinical
542 study, or larger commercial batches. As mentioned above, the scale-up of the process can be

543 performed by numbering-up the millifluidic devices. This scale-up mode ensures the production
 544 of industrial batches exhibiting similar properties to the lab-scale batches. Nevertheless, before
 545 scaling up the process and implementing it, it is important to complete the study. Indeed, the
 546 preliminary tests presented in this study have demonstrated the feasibility of the process,
 547 however they must be completed and deepened to develop conditions to observe a significant
 548 decrease of the lamina during cells essays. These new tests will be particularly important to
 549 adapt the RNA concentration in the formulations.

550



551

552 Fig. 6: Average results of Western blot quantification of lamin A for three transfection agents (JetPrime; INTERFERin and
 553 supercritical processed liposomes)

554 5. Conclusion

555 The continuous millifluidic process allows the formation of liposomes with MD ranging
 556 between 123.9 ± 3.0 nm and 165.7 ± 1.6 nm depending on the studied experimental conditions.
 557 The optimal operating conditions for the formation of liposomes with low MD were found to
 558 be 150 bar, 35°C with a phospholipid mass ratio of 0.1 wt% in the feed solution (in the operating
 559 area studied). The formed liposomes are distributed in a unimodal population with a PDI of
 560 0.24 with average diameters of 125 nm. It is therefore possible to consider this process for the
 561 formation of liposomes in gene therapy (application of liposomes with diameters below 150
 562 nm). The millifluidic process optimization studies concluded that the most influential parameter
 563 for controlling the characteristics of the liposomes formed is the phospholipid mass ratio in the
 564 feed solution. Pressure does not significantly influence the liposomes size (MD) but it has an
 565 impact on size distribution of liposomes (PDI) in liposomal suspension (higher pressure results
 566 in tighter size distribution). The millifluidic process was applied for the encapsulation of
 567 siRNAs in order to develop a potential new therapy for the treatment of progeria. The resulting
 568 formulations were compared to commercial transfection agents *ex vivo* by measuring lamin A
 569 expression by WB. These first results show that the liposomes prepared in supercritical medium
 570 containing siRNAs targeting *LMNA* allow a decrease in the expression of lamin A (major goal
 571 – decrease not yet significant for these feasibility tests). Moreover, the liposomes developed in
 572 the framework of this study are not damaging to cells in culture and seem to be safer than the
 573 commercial transfection agents generally used for this type of transfection.

574

- 575 [1] C.D. Novina, P.A. Sharp, The RNAi revolution, *Nature*. 430 (2004) 161–164.
576 <https://doi.org/10.1038/430161a>.
- 577 [2] R. Wilson, J.A. Doudna, Molecular mechanisms of RNA interference, *Annu Rev*
578 *Biophys.* 42 (2013) 217–239. <https://doi.org/10.1146/annurev-biophys-083012-130404>.
- 579 [3] M.A. Behlke, Progress towards in vivo use of siRNAs, *Mol Ther.* 13 (2006) 644–670.
580 <https://doi.org/10.1016/j.ymthe.2006.01.001>.
- 581 [4] N. Agrawal, P.V.N. Dasaradhi, A. Mohammed, P. Malhotra, R.K. Bhatnagar, S.K.
582 Mukherjee, RNA interference: biology, mechanism, and applications, *Microbiol Mol Biol*
583 *Rev.* 67 (2003) 657–685. <https://doi.org/10.1128/MMBR.67.4.657-685.2003>.
- 584 [5] I. Friedrich, A. Shir, S. Klein, A. Levitzki, RNA molecules as anti-cancer agents, *Semin*
585 *Cancer Biol.* 14 (2004) 223–230. <https://doi.org/10.1016/j.semcancer.2004.04.001>.
- 586 [6] S.K. Radhakrishnan, T.J. Layden, A.L. Gartel, RNA interference as a new strategy against
587 viral hepatitis, *Virology.* 323 (2004) 173–181. <https://doi.org/10.1016/j.virol.2004.02.021>.
- 588 [7] R.K.M. Leung, P.A. Whittaker, RNA interference: from gene silencing to gene-specific
589 therapeutics, *Pharmacol Ther.* 107 (2005) 222–239.
590 <https://doi.org/10.1016/j.pharmthera.2005.03.004>.
- 591 [8] Y. Zeng, B.R. Cullen, RNA interference in human cells is restricted to the cytoplasm.,
592 *RNA.* 8 (2002) 855–860.
- 593 [9] I.R. Gilmore, S.P. Fox, A.J. Hollins, M. Sohail, S. Akhtar, The design and exogenous
594 delivery of siRNA for post-transcriptional gene silencing, *J Drug Target.* 12 (2004) 315–
595 340. <https://doi.org/10.1080/10611860400006257>.
- 596 [10] S. Akhtar, I.F. Benter, Nonviral delivery of synthetic siRNAs in vivo, *J Clin Invest.*
597 117 (2007) 3623–3632. <https://doi.org/10.1172/JCI33494>.
- 598 [11] M. Çağdaş, A.D. Sezer, S. Bucak, Liposomes as Potential Drug Carrier Systems for
599 Drug Delivery, *Application of Nanotechnology in Drug Delivery.* (2014).
600 <https://doi.org/10.5772/58459>.
- 601 [12] J. Halder, A.A. Kamat, C.N. Landen, L.Y. Han, S.K. Lutgendorf, Y.G. Lin, W.M.
602 Merritt, N.B. Jennings, A. Chavez-Reyes, R. Coleman, D.M. Gershenson, R. Schmandt,
603 S.W. Cole, G. Lopez-Berestein, A.K. Sood, Erratum: Focal adhesion kinase targeting
604 using in vivo short interfering RNA delivery in neutral liposomes for ovarian carcinoma
605 therapy (*Clin Cancer Res* (2019) 12(4916–4924)Doi:10.1158/1078-0432.CCR-06-0021)
606 SMASH, *Clinical Cancer Research.* 25 (2019) 3194. <https://doi.org/10.1158/1078-0432.CCR-19-1132>.
- 608 [13] D.V. Morrissey, J.A. Lockridge, L. Shaw, K. Blanchard, K. Jensen, W. Breen, K.
609 Hartsough, L. Machermer, S. Radka, V. Jadhav, N. Vaish, S. Zinnen, C. Vargeese, K.
610 Bowman, C.S. Shaffer, L.B. Jeffs, A. Judge, I. MacLachlan, B. Polisky, Potent and
611 persistent in vivo anti-HBV activity of chemically modified siRNAs, *Nat Biotechnol.* 23
612 (2005) 1002–1007. <https://doi.org/10.1038/nbt1122>.
- 613 [14] S. Jafari, S. Maleki Dizaj, K. Adibkia, Cell-penetrating peptides and their analogues as
614 novel nanocarriers for drug delivery, *Bioimpacts.* 5 (2015) 103–111.
615 <https://doi.org/10.15171/bi.2015.10>.
- 616 [15] J. Gao, W. Liu, Y. Xia, W. Li, J. Sun, H. Chen, B. Li, D. Zhang, W. Qian, Y. Meng, L.
617 Deng, H. Wang, J. Chen, Y. Guo, The promotion of siRNA delivery to breast cancer
618 overexpressing epidermal growth factor receptor through anti-EGFR antibody

- 619 conjugation by immunoliposomes, *Biomaterials*. 32 (2011) 3459–3470.
620 <https://doi.org/10.1016/j.biomaterials.2011.01.034>.
- 621 [16] J.-Y. Fang, T.-L. Hwang, Y.-L. Huang, Liposomes as Vehicles for Enhancing Drug
622 Delivery Via Skin Routes, *Current Nanoscience*. 2 (2006) 55–70.
- 623 [17] G. Bozzuto, A. Molinari, Liposomes as nanomedical devices, *Int J Nanomedicine*. 10
624 (2015) 975–999. <https://doi.org/10.2147/IJN.S68861>.
- 625 [18] A. Akinc, M.A. Maier, M. Manoharan, K. Fitzgerald, M. Jayaraman, S. Barros, S.
626 Ansell, X. Du, M.J. Hope, T.D. Madden, B.L. Mui, S.C. Semple, Y.K. Tam, M. Ciufolini,
627 D. Witzigmann, J.A. Kulkarni, R. van der Meel, P.R. Cullis, The Onpattro story and the
628 clinical translation of nanomedicines containing nucleic acid-based drugs, *Nat.*
629 *Nanotechnol.* 14 (2019) 1084–1087. <https://doi.org/10.1038/s41565-019-0591-y>.
- 630 [19] J. Wang, J.D. Byrne, M.E. Napier, J.M. DeSimone, More Effective Nanomedicines
631 through Particle Design, *Small*. 7 (2011) 1919–1931.
632 <https://doi.org/10.1002/sml.201100442>.
- 633 [20] A.D. Bangham, Properties and Uses of Lipid Vesicles: An Overview, *Annals of the*
634 *New York Academy of Sciences*. 308 (1978) 2–7. [https://doi.org/10.1111/j.1749-](https://doi.org/10.1111/j.1749-6632.1978.tb22010.x)
635 [6632.1978.tb22010.x](https://doi.org/10.1111/j.1749-6632.1978.tb22010.x).
- 636 [21] B. Maherani, E. Arab-Tehrany, M. R. Mozafari, C. Gaiani, M. Linder, Liposomes: A
637 Review of Manufacturing Techniques and Targeting Strategies, *CNANO*. 7 (2011) 436–
638 452. <https://doi.org/10.2174/157341311795542453>.
- 639 [22] C.I. Nkanga, A.M. Bapolisi, N.I. Okafor, R.W.M. Krause, General Perception of
640 Liposomes: Formation, Manufacturing and Applications, *Liposomes - Advances and*
641 *Perspectives*. (2019). <https://doi.org/10.5772/intechopen.84255>.
- 642 [23] Y.P. Patil, S. Jadhav, Novel methods for liposome preparation, *Chemistry and Physics*
643 *of Lipids*. 177 (2014) 8–18. <https://doi.org/10.1016/j.chemphyslip.2013.10.011>.
- 644 [24] D.D. Lasic, Applications of Liposomes, in: *Handbook of Biological Physics*, Elsevier,
645 1995: pp. 491–519. [https://doi.org/10.1016/S1383-8121\(06\)80027-8](https://doi.org/10.1016/S1383-8121(06)80027-8).
- 646 [25] M.H.W. Milsmann, R.A. Schwendener, H.-G. Weder, The preparation of large single
647 bilayer liposomes by a fast and controlled dialysis, *Biochimica et Biophysica Acta (BBA)*
648 *- Biomembranes*. 512 (1978) 147–155. [https://doi.org/10.1016/0005-2736\(78\)90225-0](https://doi.org/10.1016/0005-2736(78)90225-0).
- 649 [26] D. Lombardo, M.A. Kiselev, Methods of Liposomes Preparation: Formation and
650 Control Factors of Versatile Nanocarriers for Biomedical and Nanomedicine Application,
651 *Pharmaceutics*. 14 (2022) 543. <https://doi.org/10.3390/pharmaceutics14030543>.
- 652 [27] T.P. Castor, Methods and apparatus for making liposomes, US5554382A, 1996.
653 <https://patents.google.com/patent/US5554382A/en> (accessed July 10, 2020).
- 654 [28] L. Frederiksen, K. Anton, P. van Hoogevest, H.R. Keller, H. Leuenberger, Preparation
655 of liposomes encapsulating water-soluble compounds using supercritical carbon dioxide,
656 *Journal of Pharmaceutical Sciences*. 86 (1997) 921–928.
657 <https://doi.org/10.1021/js960403q>.
- 658 [29] L.A. Meure, N.R. Foster, F. Dehghani, Conventional and Dense Gas Techniques for
659 the Production of Liposomes: A Review, *AAPS PharmSciTech*. 9 (2008) 798.
660 <https://doi.org/10.1208/s12249-008-9097-x>.
- 661 [30] I.E. Santo, R. Campardelli, E.C. Albuquerque, S.V. de Melo, G. Della Porta, E.
662 Reverchon, Liposomes preparation using a supercritical fluid assisted continuous process,

- 663 Chemical Engineering Journal. 249 (2014) 153–159.
664 <https://doi.org/10.1016/j.cej.2014.03.099>.
- 665 [31] L. Lesoin, C. Crampon, O. Boutin, E. Badens, Preparation of liposomes using the
666 supercritical anti-solvent (SAS) process and comparison with a conventional method, *The*
667 *Journal of Supercritical Fluids*. 57 (2011) 162–174.
668 <https://doi.org/10.1016/j.supflu.2011.01.006>.
- 669 [32] S. Kunastitchai, L. Pichert, N. Sarisuta, B.W. Müller, Application of aerosol solvent
670 extraction system (ASES) process for preparation of liposomes in a dry and
671 reconstitutable form, *International Journal of Pharmaceutics*. 316 (2006) 93–101.
672 <https://doi.org/10.1016/j.ijpharm.2006.02.051>.
- 673 [33] E. Badens, Mise en forme de principes actifs pharmaceutiques en phase supercritique,
674 *Techniques de l'ingénieur*. (2012) 24.
- 675 [34] A.D. Sandre-Giovannoli, R. Bernard, P. Cau, C. Navarro, J. Amiel, I. Boccaccio, S.
676 Lyonnet, C.L. Stewart, A. Munnich, M.L. Merrer, N. Lévy, Lamin A Truncation in
677 Hutchinson-Gilford Progeria, *Science*. (2003). <https://doi.org/10.1126/science.1084125>.
- 678 [35] K. Harhour, D. Frankel, C. Bartoli, P. Roll, A. De Sandre-Giovannoli, N. Lévy, An
679 overview of treatment strategies for Hutchinson-Gilford Progeria syndrome, *Nucleus*. 9
680 (2018) 265–276. <https://doi.org/10.1080/19491034.2018.1460045>.
- 681 [36] N. Bonello-Palot, S. Simoncini, S. Robert, P. Bourgeois, F. Sabatier, N. Levy, F.
682 Dignat-George, C. Badens, Prelamin A accumulation in endothelial cells induces
683 premature senescence and functional impairment, *Atherosclerosis*. 237 (2014) 45–52.
684 <https://doi.org/10.1016/j.atherosclerosis.2014.08.036>.
- 685 [37] Y. Murakami, K. Inoue, R. Akiyama, Y. Orita, Y. Shimoyama, LipTube: Liposome
686 Formation in the Tube Process Using Supercritical CO₂, *Ind. Eng. Chem. Res.* 61 (2022)
687 14598–14608. <https://doi.org/10.1021/acs.iecr.2c02095>.
- 688 [38] L. Lesoin, C. Crampon, O. Boutin, E. Badens, Development of a continuous dense gas
689 process for the production of liposomes, *The Journal of Supercritical Fluids*. 60 (2011)
690 51–62. <https://doi.org/10.1016/j.supflu.2011.04.018>.
- 691 [39] I. Söderberg, Phase behavior and structure in the soybean phosphatidylcholine-
692 ethanol-water system, in: B. Lindman, J.B. Rosenholm, P. Stenius (Eds.), *Surfactants and*
693 *Macromolecules: Self-Assembly at Interfaces and in Bulk*, Steinkopff, Darmstadt, 1990:
694 pp. 285–289. <https://doi.org/10.1007/BFb0118270>.
- 695 [40] L. Lesoin, O. Boutin, C. Crampon, E. Badens, CO₂/water/surfactant ternary systems
696 and liposome formation using supercritical CO₂: A review, *Colloids and Surfaces A:*
697 *Physicochemical and Engineering Aspects*. 377 (2011) 1–14.
698 <https://doi.org/10.1016/j.colsurfa.2011.01.027>.
- 699 [41] N.E. Durling, O.J. Catchpole, S.J. Tallon, J.B. Grey, Measurement and modelling of
700 the ternary phase equilibria for high pressure carbon dioxide–ethanol–water mixtures,
701 *Fluid Phase Equilibria*. 252 (2007) 103–113. <https://doi.org/10.1016/j.fluid.2006.12.014>.
- 702 [42] L. Zhao, F. Temelli, Preparation of liposomes using supercritical carbon dioxide via
703 depressurization of the supercritical phase, *Journal of Food Engineering*. 158 (2015) 104–
704 112. <https://doi.org/10.1016/j.jfoodeng.2015.03.004>.
- 705 [43] E. Reverchon, G. Della Porta, M.G. Falivene, Process parameters and morphology in
706 amoxicillin micro and submicro particles generation by supercritical antisolvent

707 precipitation, The Journal of Supercritical Fluids. 17 (2000) 239–248.
708 [https://doi.org/10.1016/S0896-8446\(00\)00045-0](https://doi.org/10.1016/S0896-8446(00)00045-0).
709
710

Journal Pre-proof

Declaration of interests

The authors declare that they have no known competing financial interests or personal relationships that could have appeared to influence the work reported in this paper.

The authors declare the following financial interests/personal relationships which may be considered as potential competing interests:

Dear editorial board of the Journal of Drug Delivery Science and Technology,

Please find enclosed the manuscript: **“Supercritical millifluidic process for siRNA encapsulation in nanoliposomes for potential Progeria treatment (ex-vivo assays)”**, by Mathieu Martino *et al.*, to be submitted as an original research in the Journal of Drug Delivery Science and Technology for consideration of publication. All co-authors have seen and agree with the contents of the manuscript. We certify hereby that the submission is original work and is not under review at any other publication. We declare that we do not have any conflicts of interest to declare.

Sincerely yours,

Mathieu Martino on behalf of the authors.

Corresponding author: Mathieu Martino, Email address: mathieu.martino@univ-amu.fr, Tel: +336 95 27 19 59

Declaration of interests

The authors declare that they have no known competing financial interests or personal relationships that could have appeared to influence the work reported in this paper.

The authors declare the following financial interests/personal relationships which may be considered as potential competing interests:

Dear editorial board of the Journal of Drug Delivery Science and Technology,

Please find enclosed the manuscript: **“Supercritical millifluidic process for siRNA encapsulation in nanoliposomes for potential Progeria treatment (ex-vivo assays)”**, by Mathieu Martino *et al.*, to be submitted as an original research in the Journal of Drug Delivery Science and Technology for consideration of publication. All co-authors have seen and agree with the contents of the manuscript. We certify hereby that the submission is original work and is not under review at any other publication. We declare that we do not have any conflicts of interest to declare.

Sincerely yours,

Mathieu Martino on behalf of the authors.

Corresponding author: Mathieu Martino, Email address: mathieu.martino@univ-amu.fr, Tel: +336 95 27 19 59